Supplementary Information (SI) for Nanoscale.
This journal is © The Royal Society of Chemistry 2026

Supporting Information For:

Thermoelectrochemistry-Enabled phase and morphology control of metal phosphide nanocrystals

Hyokyum Ahn,[a] Yunwoo Nam,[a] Taeyeon Kang,[a] Hyun S. Ahn*[a]

[a] *Department of Chemistry, Yonsei University, Seoul, 03722, Republic of Korea*

E-mail: ahnhs@yonsei.ac.kr

Table of Contents **Page**

Possible Electrochemical deposition process. The electrochemical deposition process of metal phosphides is reported to proceed via the following mechanism, as demonstrated in previous studies.[1,2,3]

Pathway 1: Direct phosphide formation via phosphine

$M^{n+} + n\ e^- \rightarrow M$

$H_2PO_2^- + 5H^+ + 4e^- \rightarrow PH_3 + 2H_2O$

$M + PH_3 \rightarrow MP + 3H^+$

Pathway 2: Sequential phosphorus reduction and alloy formation

$M^{n+} + n\ e^- \rightarrow M$

$H_2PO_2^- + 2\ H^+ + e^- \rightarrow P + 2\ H_2O$

$M + P \rightarrow MP$

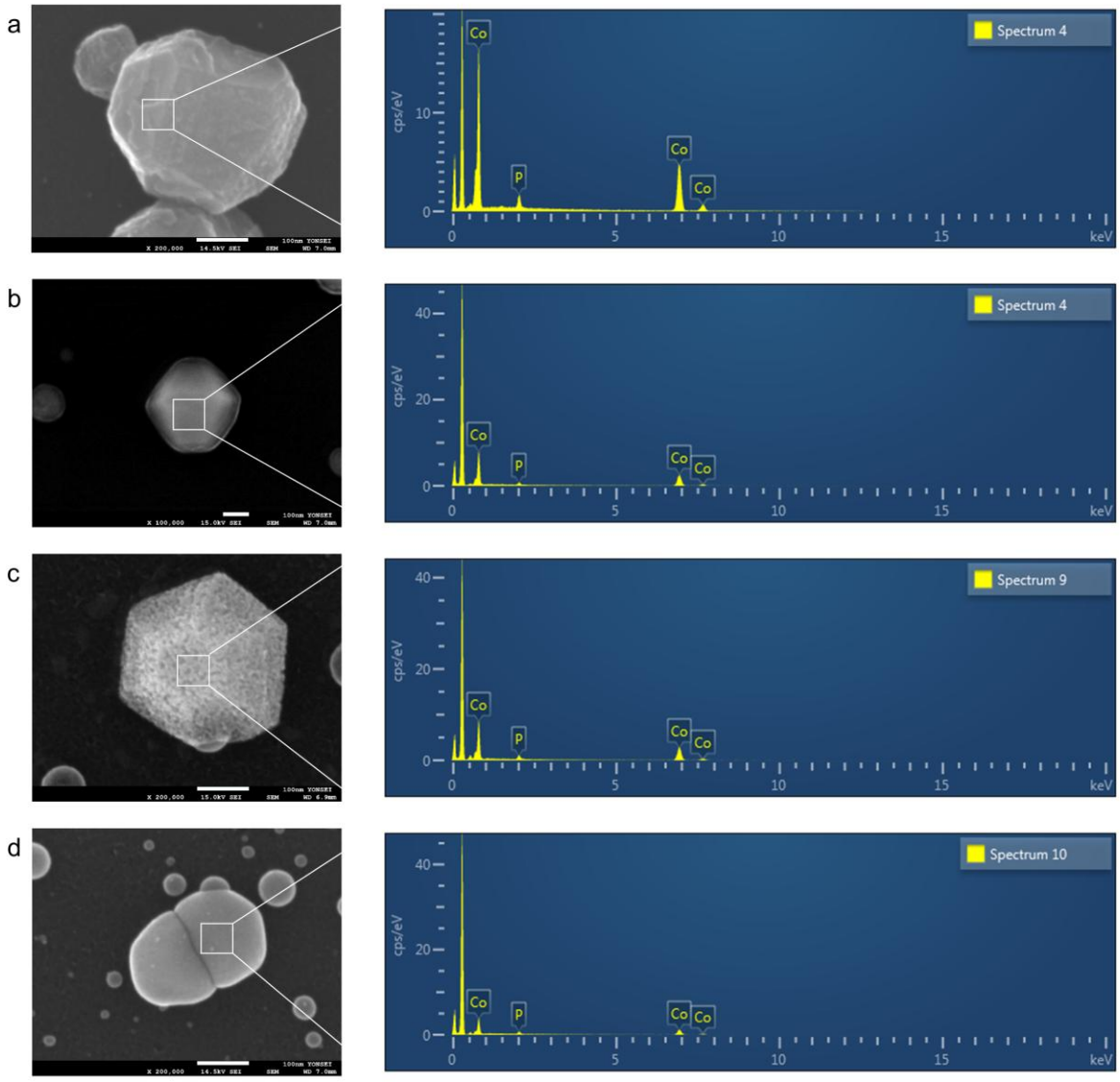

Figure. S1: Experimental results were obtained by systematically increasing the phosphorus precursor ratio under varied solution conditions, with the potential fixed at –1.15 V and heating applied for 100 seconds. The precursor ratios for cobalt and phosphorus from samples a to d were as follows: 10 mM: 100 mM, 10 mM: 500 mM, 10 mM: 1 M, and 10 mM: 5 M, respectively. Energy-dispersive X-ray spectroscopy (EDS) analysis of the corresponding particles is summarized in Table S1, showing the atomic percentages of cobalt and phosphorus present in each sample.

Element Atomic %	Fig. S1a	Fig. S1b	Fig. S1c	Fig. S1d
P	2.26	5.73	8.38	11.41
Co	97.74	94.27	91.62	88.59
Total:	100.00	100.00	100.00	100.00

Table S1. At lower phosphorus incorporation (Fig. S1a-c 2.26–8.38 at.% P), the resulting structures predominantly exhibited truncated hexagonal pyramid morphologies, indicative of phosphorus incorporation into the cobalt crystal lattice without disrupting its long-range order. But further increased phosphorus incorporation (Fig. S1d: >10 at.% P) led to a consistent transition towards amorphous morphologies. This behavior suggests a critical phosphorus loading threshold (~10 atomic %) above which crystalline Co–P nanostructures lose their ordered lattice and become amorphous.

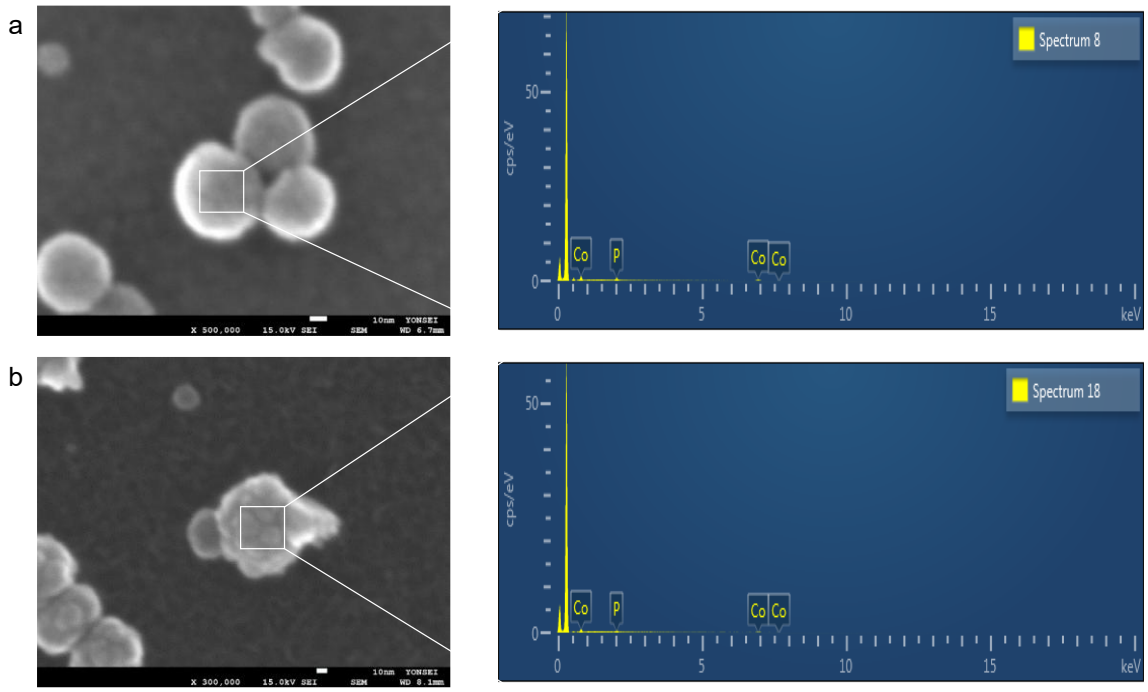

Figure S2. (a) (a) was prepared following the Figure S1 protocol, with solution conditions of 0.1 mM Co and 5 M phosphorus precursor. (b) synthesized via linear sweep voltammetry (LSV), shows polycrystalline regions. Energy-dispersive X-ray spectroscopy (EDS) analysis of the corresponding particles is summarized in Table S2, showing the atomic percentages of cobalt and phosphorus present in each sample.

Element Atomic %	Fig. S2a	Fig. S2b
P	34.85	33.99
Co	65.15	66.01
Total:	100.00	100.00

Table S2. EDS Atomic percentage of cobalt and phosphorus present in each sample.

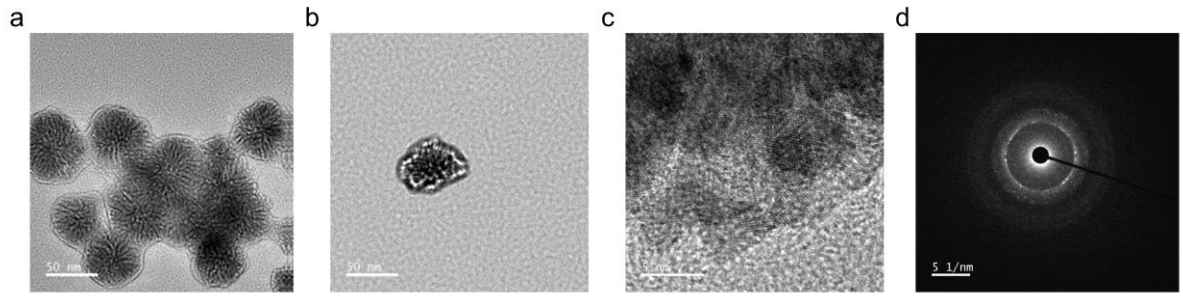

Figure S3. (a)~(d) When temperature conditions are excluded during the synthesis phase, samples synthesized under otherwise identical conditions consistently exhibit polycrystalline morphologies.

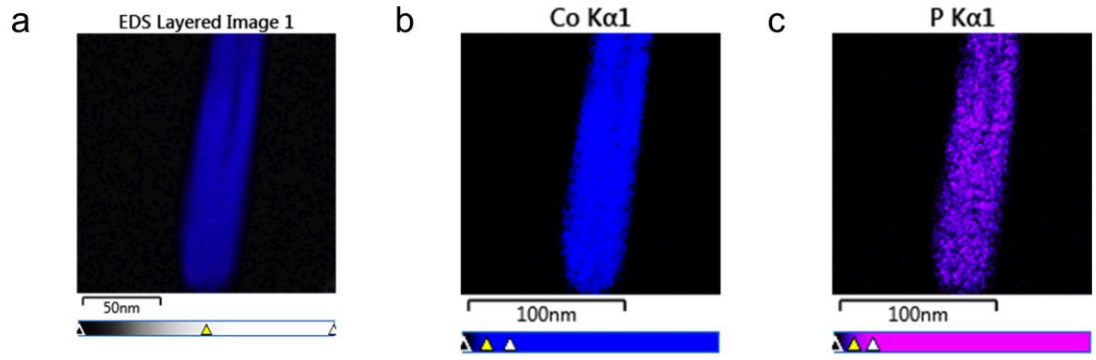

Figure S4. EDS Mapping for Fig 1.d (a) Total map (b) Co (c) P

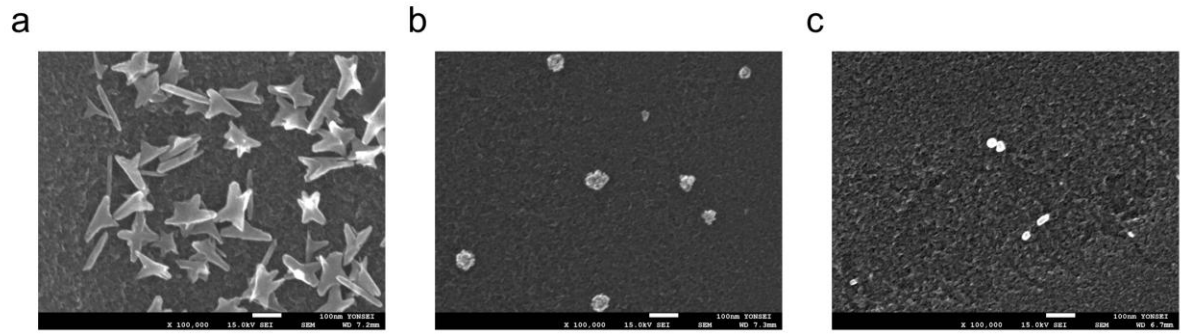

Figure S5. All samples were synthesized according to the protocol described for Fig. 2, with the applied step potential (E step) systematically varied as follows: (a) –1.05 V; (b): –1.03 V; (c) : –0.9 V.

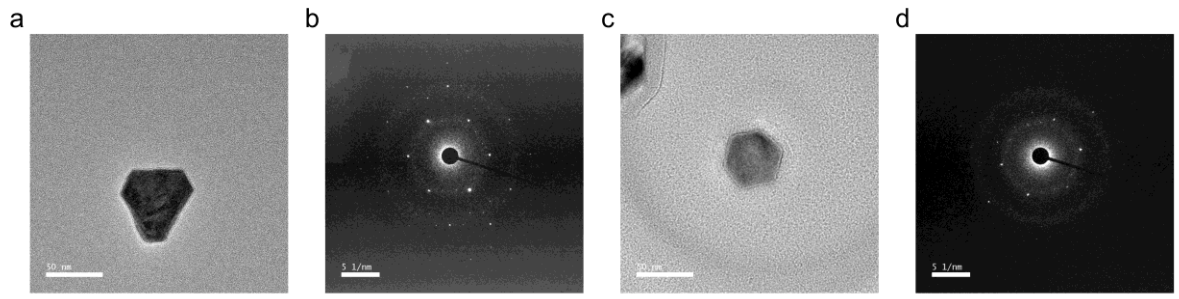

Figure S6. Representative Ni_2P morphologies: (a) Nearly triangular hexagonal platelet,(b) Single-crystal SAED pattern of (a), (c) Hexagonal platelet-type particle, (d) Single-crystal SAED pattern of (c).

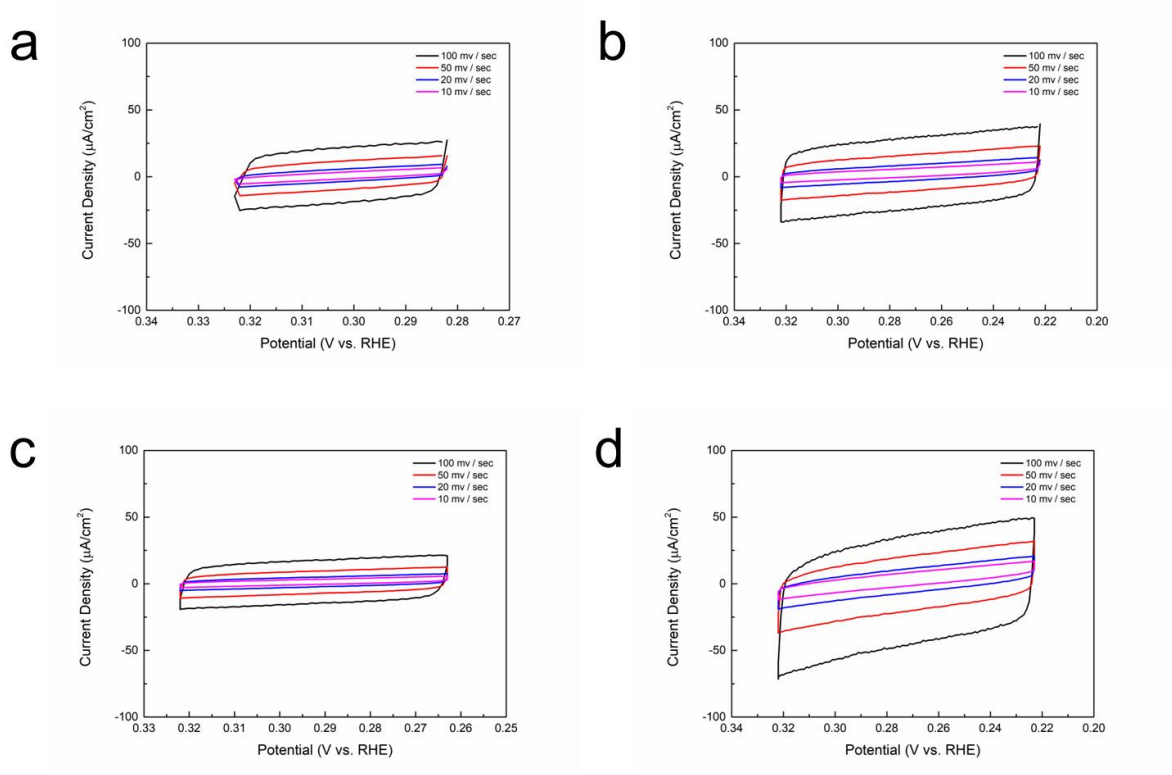

Figure S7. Non-Faradaic capacitance plots at various scan rates for H_2SO_4 solution (a) HER rod, (b) HER Bundle, (c) OER rod, (d) OER Bundle

These data were used in computing the electrochemical surface area (ECSA) values for the different samples using the formula $ECSA=C_{dl}/C_s$, where Cs is the specific capacitance. A C_s value of 0.04 mF/cm^2 was referenced from previous studies.[4]

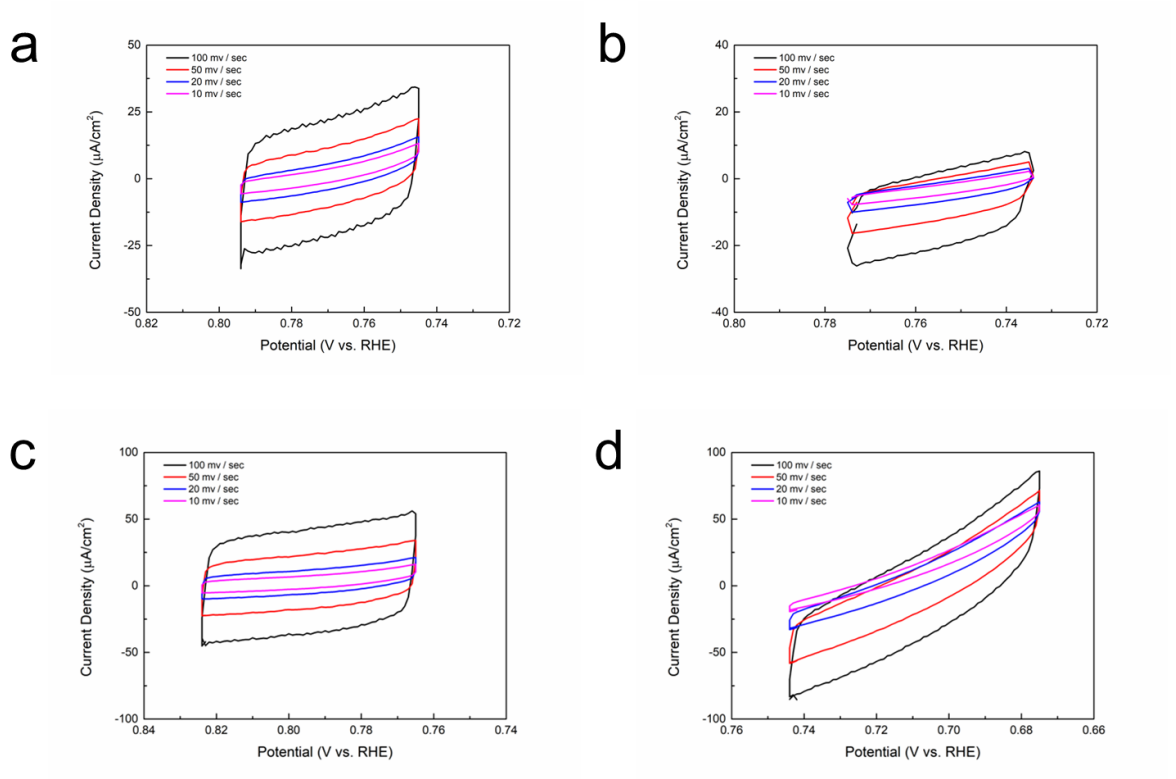

Figure S8. Non-Faradaic capacitance plots at various scan rates for 1M KOH solution (a) HER rod, (b) HER Bundle, (c) OER rod, (d) OER Bundle

References

(1) N. Shida, J. A. Buss and T. Agapie, Chem. Commun., 2018, 54, 767–770.

(2) C. Wang, Y. Wu, Z. Zhou, J. Wang, S. Pei and S. Liu, International Journal of Hydrogen Energy, 2022, 47, 40849–40859.

(3) Z. Lu and L. Sepunaru, Electrochimica Acta, 2020, 363, 137167.

(4) S. I. Mutinda, T. N. Batugedara, B. Brown and S. L. Brock, *ChemCatChem*, 2021, **13**, 4111–4119.